remote sensing

MDPI

Article

Tropical Texture Determination by Proximal Sensing Using a Regional Spectral Library and Its Relationship with Soil Classification

Marilusa P. C. Lacerda [1], José A. M. Demattê [2,*], Marcus V. Sato [2], Caio T. Fongaro [2], Bruna C. Gallo [2] and Arnaldo B. Souza [2]

[1] Faculty of Agronomy and Veterinary Medicine, University of Brasilia; Campus Universitário Darcy Ribeiro, ICC Sul, Asa Norte, Postal Box 4508, Brasília 70910-960, Brazil; marilusa@unb.br

[2] Department of Soil Science, College of Agriculture Luiz de Queiroz, University of São Paulo; Pádua Dias Av., 11, Piracicaba, Postal Box 09, São Paulo 13416-900, Brazil; satomarcusvinicius@gmail.com (M.V.S.); caio.fongaro@gmail.com (C.T.F.); gallo.bruna@gmail.com (B.C.G.); souza.arnaldobarros@usp.br (A.B.S.)

* Correspondence: jamdemat@usp.br; Tel.: +55-19-3417-2109

Academic Editors: Lenio Soares Galvao, Xiaofeng Li and Prasad S. Thenkabail
Received: 22 March 2016; Accepted: 17 August 2016; Published: 26 August 2016

Abstract: The search for sustainable land use has increased in Brazil due to the important role that agriculture plays in the country. Soil detailed classification is related with texture attribute. How can one discriminate the same soil class with different textures using proximal soil sensing, as to reach surveys, land use planning and increase crop productivity? This study aims to evaluate soil texture using a regional spectral library and its usefulness on classification. We collected 3750 soil samples covering 3 million ha within strong soil class variations in São Paulo State. The spectral analyses of soil samples from topsoil and subsoil were measured in laboratory (400–2500 nm). The potential of a regional soil spectral library was evaluated on the discrimination of soil texture. We considered two types of soil texture systems, one related with soil classification and another with soil managements. The soil line technique was used to assess differentiation between soil textural groups. Soil spectra were summarized by principal component analysis (PCA) to select relevant information on the spectra. Partial least squares regression (PLSR) was used to predict texture. Spectral curves indicated different shapes according to soil texture and discriminated particle size classes from clayey to sandy soils. In the visible region, differences were small because of the organic matter, while the short wave infrared (SWIR) region showed more differences; thus, soil texture variation could be differentiated by quartz. Angulation differences are on a spectral curve from NIR to SWIR. The statistical models predicted clay and sand levels with R^2 = 0.93 and 0.96, respectively. Indeed, we achieved a difference of 1.2% between laboratory and spectroscopy measurement for clay. The spectral information was useful to classify Ferralsols with different texture classification. In addition, the spectra differentiated Lixisols from Ferralsols and Arenosols. This work can help the development of computer programs that allow soil texture classification and subsequent digital soil mapping at detailed scales. In addition, it complies with requirements for sustainable land use and soil management.

Keywords: remote sensing; proximal sensing; soils attributes; sustainable land use; soils survey and mapping; digital soil mapping; soil management; chemometrics; spectroscopy

1. Introduction

Brazil is one of the world's largest producers of agricultural goods. Sustainable land use is the basis to ensure soil quality. The increasing demand for food and renewable energy sources has required intensive land use, which in turn promotes disorderly land occupation, often driven by economic factors. This occupation may affect soil quality and compromise its potential for agricultural use.

Thus, detailed knowledge of pedological classes through mapping associated with climate information plays an important role in land use planning. This information provides the basis for the development of agricultural projects by identifying suitable areas for agricultural crops and contributing to soil conservation. In addition, it gives technical classification of soils (agricultural capacity, and land use capacity) [1].

In Brazil, the existing soil maps were based on exploratory or recognition levels, with few areas surveyed with large scale. In fact, Mendonça Santos and Santos [2] indicate that soil surveys at semi-detailed to detailed levels correspond to approximately 0.25% of the Brazilian territory.

New pedological mapping techniques have evolved in recent years, following the evolution of soil classification systems in Brazil [3,4] and the world [5]. Among the new techniques used, remote sensing (RS) stands out as an auxiliary tool in soil recognition at land [6], aerial and orbital levels [7]. The spectral behavior of soils is directly linked to its chemical, physical, biological and mineralogical composition, where contents of organic matter (OM) and iron oxides, mineralogy of the clay fraction, in addition to the particle size and moisture, influence spectral responses [8]. In this respect, the soil has also been studied by a technique called Proximal Sensing (PS) [9]. Proximal Soil Sensing refers to data acquisition from the development of sampling schemes and high resolution sensor data.

Remote sensing has been used in various fields of study in soil science, such as quantification of attributes [6,10–18], among others. A recent literature review performed by Soriano-Disla et al. [19] indicates several works in this field.

Spectral studies require data organization at regional or continental levels through spectral libraries for optimization. Efforts have been made to develop spectral libraries in Brazil [20] and the world. An example is the preliminary spectral library of soils organized by Van Reeuwjik [21] in various countries (Africa, Asia, Europe, North America and South America) that used spectral data of soils in the Soil Information System (ISIS) of the International Soil Reference and Information Centre (ISRIC). Subsequently, Viscarra Rossel and Webster [22] developed a spectral library of soils of the Australian continent. The USDA [23] organized the library of North American soils and Stevens et al. [24] produced the library for European soils, named LUCAS. However, as indicated by Nocita et al. [25], these libraries can be optimized through a suitable treatment of spectral data in laboratories.

From several soil attributes, texture is one of the most important one, since it plays with water and chemical elements. In addition, this attribute is used for soil classification. Usually, it is determined by the particle size analysis traditionally performed in laboratories. Nevertheless, demand for data on soil attributes is increasing and requires data optimization. The soil particle size influences decisions about the proper use and handling of agricultural land. This feature can be discriminated by reflectance spectroscopy, allowing individualization of different particle size classes.

Differentiation of soil spectra through the particle size analysis can assist in determining physical and chemical properties conditioned by soil texture, such as mineralogical composition, iron oxide and OM contents, among others [6,10–18]. Clayey soils have spectra characteristically flatter in the infrared region due to the high absorption caused by iron oxides and OM. Thus, the prediction models of clay values and soil textures can assist soil characterization, classification and identification and may optimize laboratory analyses.

Due to its specificity and associations with physical and chemical attributes, soil texture is an important attribute in determining Land Use and Management Brazilian Technical Classifications (LBTC). It is well known that there are several soil attributes in soil classification, where texture is one of the most important. However, few studies have used a large database to quantify particle size fractions in tropical soils. At once, discussions on how to use these spectral libraries to achieve a soil attribute, is still under debate. Thus, assessment of soil texture by the spectroscopic analysis and soil spectral libraries can support digital mapping.

This study aimed to determine the differences between spectra related with changes in particle sizes. We evaluated soil texture classification using a regional spectral library, representing the

tropics. In addition, we aimed to generate a prediction model to quantify soil texture and evaluate its usefulness in pedological classification. This work can be used for the development of computer programs for classification of soil texture at detailed scales used in digital soil mapping, complying with requirements for sustainable land use.

2. Materials and Methods

2.1. Location of the Study Site and Sampling Points

The study site is located in São Paulo State near the municipalities of Jaboticabal and São Carlos, between the coordinates UTM (Zone 22S, Datum SIRGAS 2000) from 731,000 to 830,000 m and 7,630,000 to 7,535,000 m. The entire site was divided into Areas I, II and III by location, where Area I is in the north, Area II is in the center and Area III is in the south of the sampling site (Figure 1).

Sampling points were marked in the study site using the topossequence method in order to cover all variations of soil classes represented in the region. Traditionally, topossequence soil samples goes from higher to lower altitudes. The initial work was represented by the sampling points in the Central area, called in this work as Area II. Later, it was possible to extend the sampling points to the areas called North (Area I) and South (Area III). For this reason, some sampling points from North (Area I) are located in both areas, but with a predominance in Area II. The sampling points were geographically located through the GPS-PRO-XR sub-metric system.

The samples were collected through boreholes in all sampling points, at depths 0–0.2 m, 0.4–0.6 m and 0.8–1.0 m, duly identified and forwarded for laboratory testing. The first sampling depth corresponds to the surface horizon (A), the second depth, to the transitional horizon and the third depth, to the subsurface horizon (B) of soils. The undersurface sampling is to represent the horizon B, since this is its position in this region (about 0.8–1.00 m). Due to the variability of soil classes, 3752 samples were collected, 67 in Area I, 910 in Area II and 2775 in Area III.

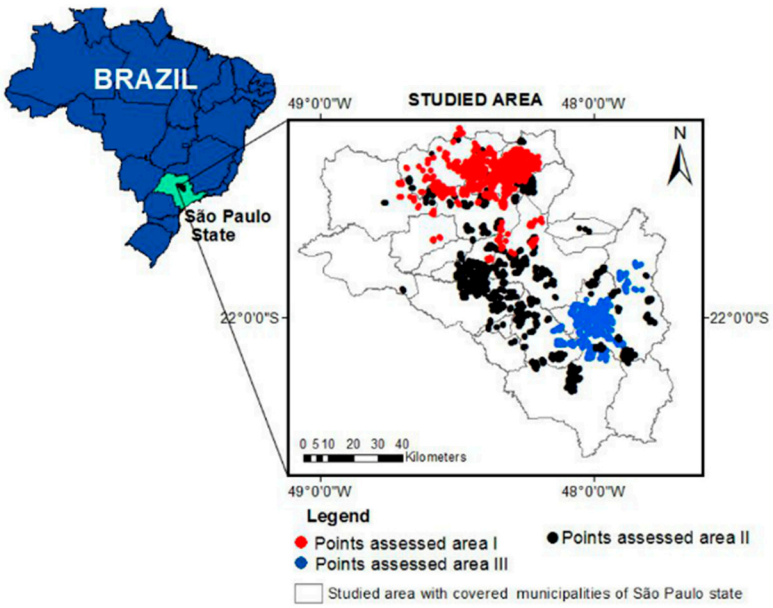

Figure 1. Location of the study site and sampling points in Areas I, II, and III.

2.2. Assessment of Textural Groups of the Soils Studied

2.2.1. Particle Size and Spectroscopic Analyses of Soil Samples

The particle size analyses (textural analysis) of the TFSA fraction of soil samples were conducted using the Densimeter Method, also known as the Bouyoucos Method [26].

Reflectance spectroscopy was performed using a Fieldspec 3 (ASD Inc., Boulder, CO, USA) sensor Inc. with spectral resolution of 1 nm, covering wavelengths between 350 nm and 2500 nm (VIS-NIR-SWIR). For data collection, samples were oven-dried at 45 °C for 24 h, milled and sieved (2 mm). Later, the samples were placed on petri dishes and distributed homogeneously on a flat surface to perform the readings. Two halogen lights (50 W) were used as light source. The lights were placed at 90° from each other, 35 cm away from the sample and Zenithal angle of 30° with non-collimated beam to the plan in question. An optic-fiber cable placed at 8 cm from the sample surface captured the light, which was measured using reflected energy over an area of approximately 2 cm^2 in the center of the sample. Reflectance for each sample was the result of the average of 100 sensor readings. The instrument was calibrated every 20 min with a white spectralon plate, calibrated at 100% reflectance.

2.2.2. Assessment of Textural Groups

The database was organized into textural groups, considering Brazilian Soil Classification System (SiBCS) [4], and according to the management land use information developed by Demattê and Demattê [1].

Based on SiBCS, the textural groups were subdivided into the following classes: (1) Sandy (clay contents < 150 $g \cdot kg^{-1}$); (2) Average (clay contents between 150 and 350 $g \cdot kg^{-1}$); (3) Clayey (clay contents between 350 and 600 $g \cdot kg^{-1}$); and (4) very clayey (clay contents > 600 $g \cdot kg^{-1}$). On the other hand, following the management practices the classes were more subdivided into: (1) Very Sandy (clay contents < 100 $g \cdot kg^{-1}$); (2) Sandy (clay contents between 100 and 150 $g \cdot kg^{-1}$); (3) Average Sandy (clay contents between 150 and 250 $g \cdot kg^{-1}$); (4) Average Clayey (clay contents between 250 and 350 $g \cdot kg^{-1}$); (5) Clayey (clay contents between 350 and 600 $g \cdot kg^{-1}$); and (6) very clayey (clay contents > 600 $g \cdot kg^{-1}$).

We averaged the spectra within each textural class for evaluation. Later, the responses were plotted on reflectance (%) vs. wavelength (nm), resulting in spectral curves of each textural class.

2.2.3. Particle Size Assessment vs. Spectral Data

The soil line is highly used to check for variations in soil characterization and conditions of environments where soils are located [27]. Some vegetation indices are based on soils exposed in a two-dimensional graph, formed by a band in the visible infrared vs. a band in the near infrared, and the indices occur approximately on a line known as the soil line. The amount of vegetation in the studied site is then proportional to the Euclidean orthogonal distance in the two-dimensional graphics mentioned above, between the vegetation and the soil line [28]. Conversely, the Euclidean distance based on vegetation indices has its orthogonal complement content related to the optical properties of soils for small amounts of vegetation [29]. Thus, reflectance values for exposed soil plotted on a two-dimensional graph, formed by a band of the electromagnetic spectrum in the visible range vs. a band in the near-infrared range, occur near the soil line. The use of the soil line as a technique for digital information processing has been quite widespread used.

Soil lines were designed to assess the differentiation between distributions of textural soil classes grouped into the SiBCS [4], and the LBTC [1]. Therefore, the XY graphs were generated, where the x-axis corresponds to the spectral response of average readings within the wavelength range equivalent to band 3 of Landsat TM (630 nm to 690 nm). The y-axis represents the spectral response of average readings within the range corresponding to band 4 of the same sensor (760 nm to 900 nm). Plotted points that are very close to the soil line indicate that the samples represent only the soil. When the dispersion of graph points is approximately within a range along 45° in relation to the x-axis with R^2 values near value 1.0, is also soil information. Another scatter plot between Landsat 5 (1550–1750 nm) and 7 (2080–2350 nm) bands was performed to evaluate differences between soil textures.

2.3. Quantitative and Descriptive Spectral Assessment

The data were evaluated in two stages: (a) descriptive assessment approach (shape, intensity and curve features) [30,31]; and (b) statistical approach, through multivariate statistical analyses.

To generate the prediction model of soil texture from the database, we performed the principal component analysis (PCA) and the partial least squares regression (PLSR), using Unscrambler software [32].

2.3.1. Assessment of Principal Component Analysis (PCA)

The soil database is composed by 3750 samples with spectral data in 2151 bands. In order to select relevant information, the data of each sample were transformed into a group of independent values using the PCA [33,34]. The PCA can determine data variability to check for existing relations of covariance within the set of original variables. Afterward the system can regroup the original data into a new and smaller set through transformations that generate new variables [35]. The main objective was to summarize the content of the original data, eliminating redundant information. This technique performs a long series of matrix operations [33].

Spectral data and contents of sand, silt and clay were transformed into the ASCII format to be imported into the Unscrambler [32]. This program offers several options for data treatment to optimize the PCA. Various treatments were tested and the sequence that better featured the results in the transformation, in accordance to Franceschini et al. [36], as follows: first, spectral transformation of reflectance data for absorbance; second, spectral data processing by SNV (Standard Normal Variate); third, transformation of spectral data by MSC (Multiple Scattering Correction); and, fourth, data smoothing by applying the Savitzky–Golay filter with second-order polynomial.

Afterwards, the PCA was conducted using the cross-validation methodology with random sampling through 20 segments with one sample per segment and the complete model with centralization of spectral data through 20 PCs (Principal Components). The PC1 and PC3 were used in the analyses where PC1 represented 62% and PC 316%, respectively, of the samples studied and the PCA with spectral data of these PCs showed better results of scores that summarize the quantification of the variations between the spectral samples and loadings, which represent parts of the spectrum where such variations occur.

2.3.2. Prediction Models for Soil Attributes

We used PLSR through the Unscrambler software applying PSL1 that matches the version of the PLSR method with only one variable [33] to generate the prediction models of clay and sand contents in the soil database. Models were developed to predict clay and sand contents to verify their effectiveness. Similar to the PCA, several treatments were tested to obtain models that were statistically significant and adjusted. We compared the performance of PLSR, evaluated by means of higher determination coefficients (R^2), standard deviation (RPD) the root of the mean square error (RMSE). After tests of treatments, the PLSR analyses were carried out by selecting the following treatments: (a) Treatment 1, no treatment of spectral data; (b) Treatment 2, transformation of the spectral data in first derivative of Savitzky–Golay + data smoothing by applying Savitzky–Golay filter; and (c) Treatment 3, spectral transformation of reflectance data for absorbance.

The calibration model was performed using 70% of the samples in the database, while 30% of were used for validation. The division of the samples in these groups was carried out randomly (Terra et al. [9]). The PLSR model was performed several times, but always using 30% of samples selected randomly by the Unscrambler. The best accuracy of the model was achieved with converging the spectral data in the main components with a higher ratio to the total of the samples studied, using 20 PCs (Principal Components).

In the model validation process, some parameters were calculated to indicate their performance, which allowed generating a model with determination coefficients (R^2), standard deviation values of the error (RPD) and values of root mean square error (RMSE) (Equations (1)–(3)).

The determination coefficient (R^2) was calculated by Equation (1):

$$R^2 = \frac{\sum_{i=1}^{n} (\hat{y}_i - \overline{y}_i)^2}{\sum_{i=1}^{n} (y_i - \overline{y}_i)^2} \quad (1)$$

where $\hat{y}_i$ is the estimated values by the model; y_i is the observed values; $\bar{y}_i$ is the average values; and n is the number of observations of model variable.

The standard deviation values of the error (RPD) were calculated by Equation (2):

$$RPD = \frac{sd}{SEP} \quad (2)$$

where sd is the standard deviation of the data analyzed; and SEP is the standard error of prediction.

The square root of the mean error (RMSE) was calculated by Equation (3):

$$RMSE = \sqrt{\frac{1}{N} \sum_{i=1}^{N} (\hat{y}_i - \overline{y}_i)^2} \quad (3)$$

where N is the number of samples used in the prediction; and $\hat{y}_i$ and y_i are the values of predicted and measured soil properties, respectively.

To assess the wavelengths with the greatest contribution to predict soil attributes, we used PLSR algorithm [33] performed in "The Unscrambler" software [32]. The software calculates a coefficient called "b", which presented a value for each spectral band. The closer to zero, the smaller the influence of the band on the statistical model, as indicated:

$$b = W(p^T \times W)^{-1} \times q \quad (4)$$

where b is the regression coefficients; W is the weight of each of the regions of the spectrum; p is the matrix of a column (loadings reflectance); and q is the matrix of a column and a row (a single value, loading the attribute.

Therefore, it is possible to develop the regression equation (Equation (5)) according to the selection of the bands.

$$Y = b_0 + \sum_{i=1}^{n} (R_i \times b_i) \quad (5)$$

where b_0 is the correction factor; R_i is the regression coefficients for each spectral region; and bi is the reflectance in each spectrum region.

Chang et al. [35], for comparison purposes, classified prediction models into three quality categories, considering the prediction reliability for the RPD (ratio of performance to deviation) values: (1) values greater than 2.0 represent excellent models that can accurately predict the attribute under evaluation; (2) values between 1.4 and 2.0 are indicative of reasonable models that can be improved; and (3) values below 1.4 correspond to unreliable models. Stenberg et al. [37] found an average value around 1.8 by evaluating several scientific studies.

2.3.3. Assessment of Attribute Prediction Model-Descriptive Statistical Analyses

Descriptive statistical analyses were performed to assess the contents of clay, silt and sand predicted by the models with Treatment 3 (PLSR3): transformation of spectral reflectance data to absorbance and PLSR with Treatment 1 (PLSR1): without treatment of spectral data for the analyzed/measured values of clay, silt and sand.

2.3.4. Ternary Diagrams of Textural Classification Ofsoils: Real vs. Espectral Values

In order to evaluate the results obtained by the prediction models for contents of clay, silt and sand, measured and predicted data were plotted. In this matter, we correlated models elaborated by the PLSR regressions with Treatment 3: PLSR3, spectral transformation of reflectance data for

absorbance; and PLSR1 with Treatment 1: without data processing for analyzed/measured values of clay, silt and sand.

2.4. Spectral Soil Classification

We determined an automatized system to classify soils by their spectral behavior. A "hyperspectral" system was used based on principal components acquired from the spectra between 350 and 2500 nm. We used the linear discriminant analysis (LDA) [38]. This method can determine linear combinations to maximize differences between soil classes. The accuracy of the models was accessed by the reclassification of observations. All analyses were processed in the R program [39]. We performed three types of analyses: (1) discrimination of Ferralsols (LV), Lixisols (PV) and Arenosols (RQ); (2) discrimination of texture classification of Ferralsols and Arenosols; and (3) discrimination of texture classification of Lixisols. For that, we inserted the spectra of soil samples from death 0–0.2 m and 0.8–1.0 m, which correspond to horizons A and B, respectively, into a spectral soil library the system.

3. Results and Discussion

3.1. Assessment of Textural Groups of the Soils Studied

The tropical soils studied showed high variation in the particle size classes with sandy to very clayey texture. In general, the soils presented low silt contents and were classified as developed soils at an advanced weathering stage. The predominance of clay or sand constituted the origin materials of these soils, which comprise diabase, gabbro and basalts of the Serra Geral Formation and sandstones of the Bauru and/or Botucatu Formation [40].

The soil samples were ordered by the simplified textural group according to SiBCS [4] and the system used in the management of land use (Figure 2a,b). The texture classes from each group were represented by the average of spectral responses from 350 to 2500 nm. Therefore, it was possible to generate individualized spectral curves for different classes and textural groupings.

The grouping of textural classes in the LBTC featured higher reflectance values for the very sandy class in comparison to the sandy one of the simplified classification in the SiBCS. This variation is due to the average values used, in SiBCS. Sandy soil classes have clay contents <150 $g \cdot kg^{-1}$; on the other hand, following the LBTC sandy classes were subdivided into Very Sandy (clay contents < 100 $g \cdot kg^{-1}$) and Sandy (clay contents between 100 and 150 $g \cdot kg^{-1}$). When reflectance of soils with clay content is >100 $g \cdot kg^{-1}$ and >150 $g \cdot kg^{-1}$, the average reflectance values are diluted and give a false interpretation that the highest reflectance value of sandy soils is roughly 0.35%, while in classes of individual texture in very sandy and sandy management systems, reflectance values are greater than 0.40%. These high reflectance values are associated with the mineralogical constitution of sandy and very sandy soils, where quartz is the main mineral in the sand fraction. Quartz is a mineral with low absorption and consequently presents high reflectance of electromagnetic radiation.

Clayey and very clayey classes, with equal clay content in both groups, showed low reflectance values of about 12%. This is due to the mineralogical composition of these soils with occurrence of Fe oxides. The soil classes occurring in the study site showed differences in the evolution degree, which reflects directly on silicate soil mineralogy. In fact, very clayey soils are the most developed ones (Ferralsols = Latosols) because the morphology of spectral curves shows predominance of Fe oxides, kaolinite and gibbsite (Figure 2). Medium-textured soils, in turn, present more developed water absorption peaks. In sandy soils, water peaks are also pronounced, showing clay-mineral association 1:1 or hygroscopic minerals.

The textural grouping adopted by management systems, which encompass six classes of soil texture (Figure 2b), is the most indicated for planning sustainable agricultural activities. The individualization of more textural classes reflect distinct soil behaviors for land use and occupation and for the adoption of techniques for soil and water conservation. Although more than two textural classes were created, they were duly differentiated.

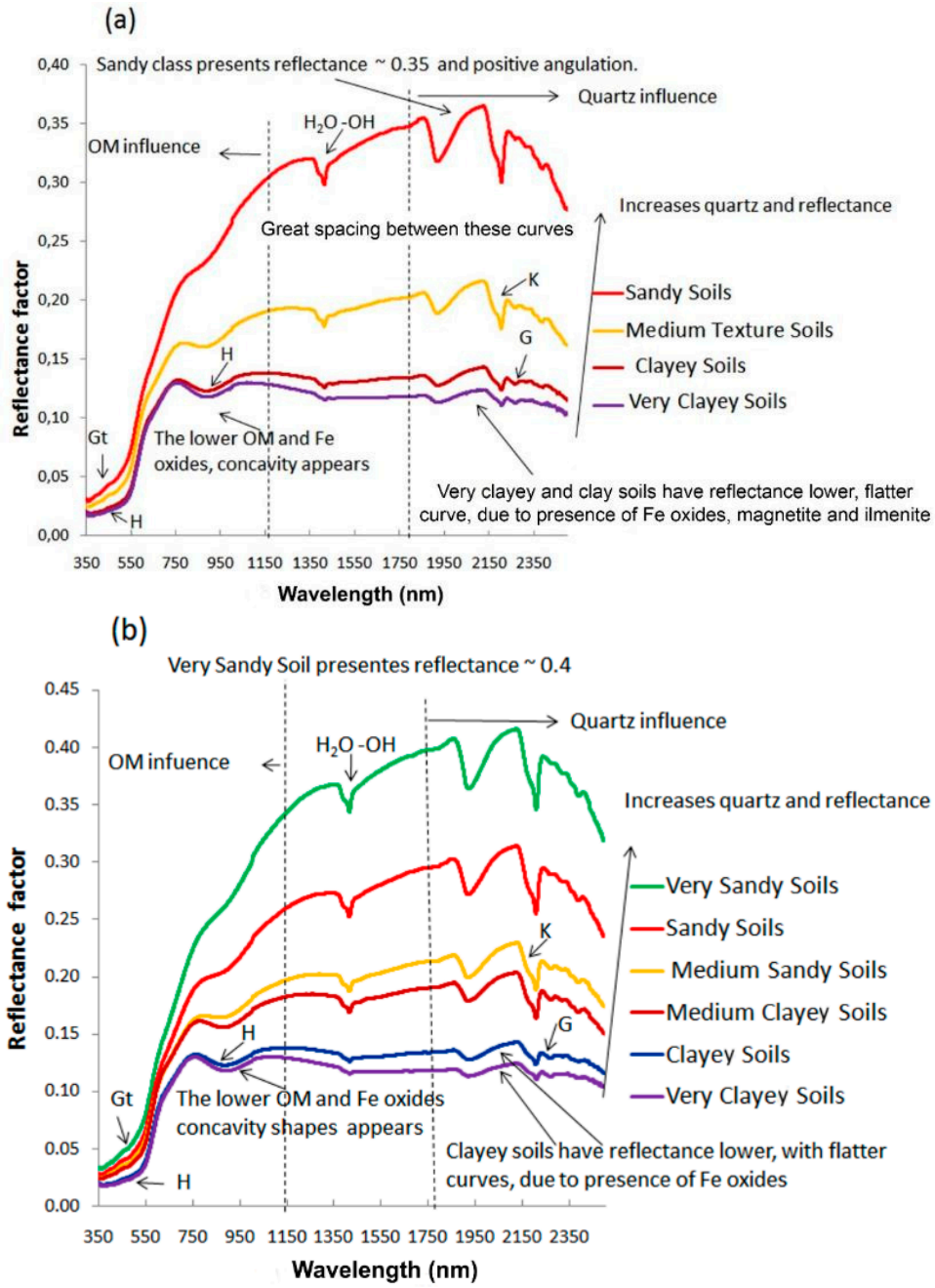

Figure 2. (**a**) Spectral curves of the studied soils individualized for simplified textural groupings SiBCS and (**b**) textural groupings in LBTC: K, kaolinite; G, gibbsite; H, hematite; and Gt, goethite.

The behavior of the spectral curves (Figure 2a,b) according to texture showed features similar to those described by Stoner and Baumgardner [41] and Demattê [30]. As the sample contains less clay and silt, and is, therefore, sandier, there is an increase in reflectance in SWIR. This is due to the presence of quartz that reflects energy within this band [20,30,36,41]. Throughout the spectrum, particularly in the VIS-NIR range, reflectance remains low, due to the presence of OM and Fe oxides that absorb energy in this range.

The angular variation (Figure 3a) advocated by Demattê [30] showed the angular change along the spectra (VIS-NIR-SWIR) caused by the double action of OM + Fe oxides (VIS) and quartz (NIR-SWIR). In Figure 3b, spectral curves of a very sandy and a very clayey soil sample were resampled to the spectral resolution of the Landsat TM 5 sensor for illustration.

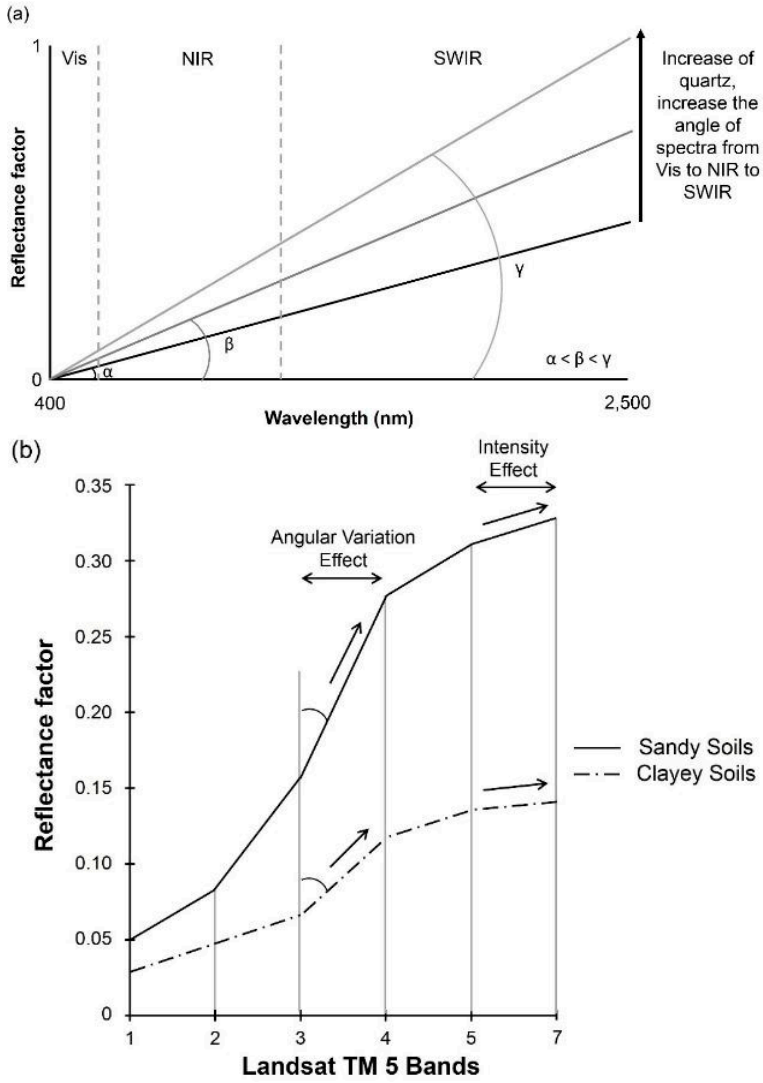

Figure 3. (**a**) Illustrative scheme of angular change of the spectral curves as a function of clay content and quartz increase in the sand fraction; and (**b**) angular change in the region of Visible to Near Infrared (TM3 and TM4 Landsat bands, respectively) in sandy and clayey soils.

Spectroscopic Analyses of Soil Samples

The soil line is a spectral evaluation method widely used to verify if the soil is bare [42–44]. The method preconizes a scatter plot between bands 3 and 4 of Landsat TM 5 (Figure 4a,b) as well as between bands 5 and 7 (Figure 5a,b). Figure 3b presents the angular alteration due to granulometric variation, allows understanding how soil attributes may present variations in the representative graph of reflectance vs. wavelength. A sandy soil displays greater variation between bands 3 and 4, while is lower for clayey soils. Bands 5 and 7, in turn, do not cause angular changes, but cause intensity alterations.

Resampled spectra in the soil line via bands 3 and 4 (Figure 4a,b) feature presents angular variation from clayey to sandy soils, and are also described by Demattê [30] and Nanni and Demattê [44]. This occurred both in the group classification of SiBCS [4] and Land Use and Management Brazilian Technical Classifications. On the other hand, the greater specification of particle size in the LBTC showed better spectral discrimination of its textural classes. The angular variation is related to quartz action at the end of the visible band, in accordance to Nanni and Demattê [44], for tropical soils.

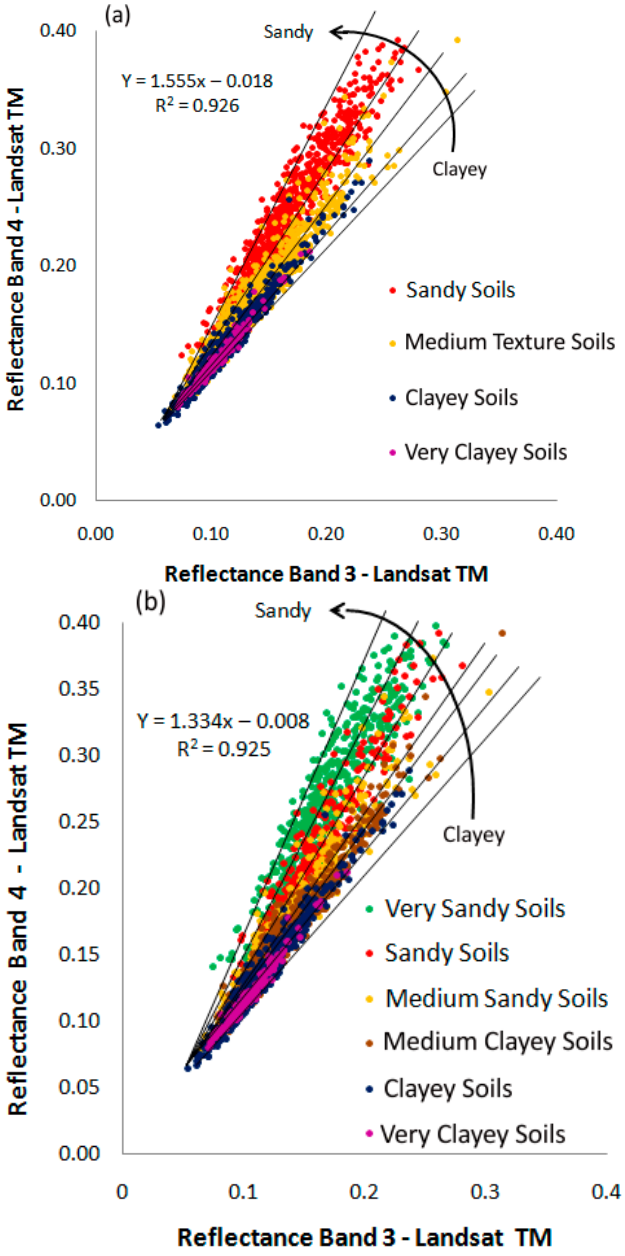

Figure 4. Soil lines obtained for the soils studied through laboratory data simulating TM3 and TM4 bands: (**a**) distribution of textural classes according to the grouping for simplified classification according to SiBCS and (**b**) distribution of textural classes according to the grouping in LBTC.

Clayey soils are positioned at the bottom of the chart (Figure 4a,b and Figure 5a,b). This is because these soils feature have smaller particles, which reflect less energy, in addition to greater energy absorbed by the components of this fraction (mainly Fe oxides). In contrast, samples with less clay and more sand reflect more and they are placed at the top of the chart, as reported by Stoner and Baumgardner [41] and Demattê [30] (Figure 4a,b and Figure 5a,b).

The use of two SWIR bands (5 and 7) provided better results than the soil line using bands 3 and 4 of Landsat. This is attributed to the greater sensitivity of spectral response within these wavelength ranges, since band 5 represents mainly the moisture content of vegetation and soils, while band 7 features sensitivity to terrain morphology providing information on the substrate (soil and geology), allowing identifying minerals with hydroxyl ions.

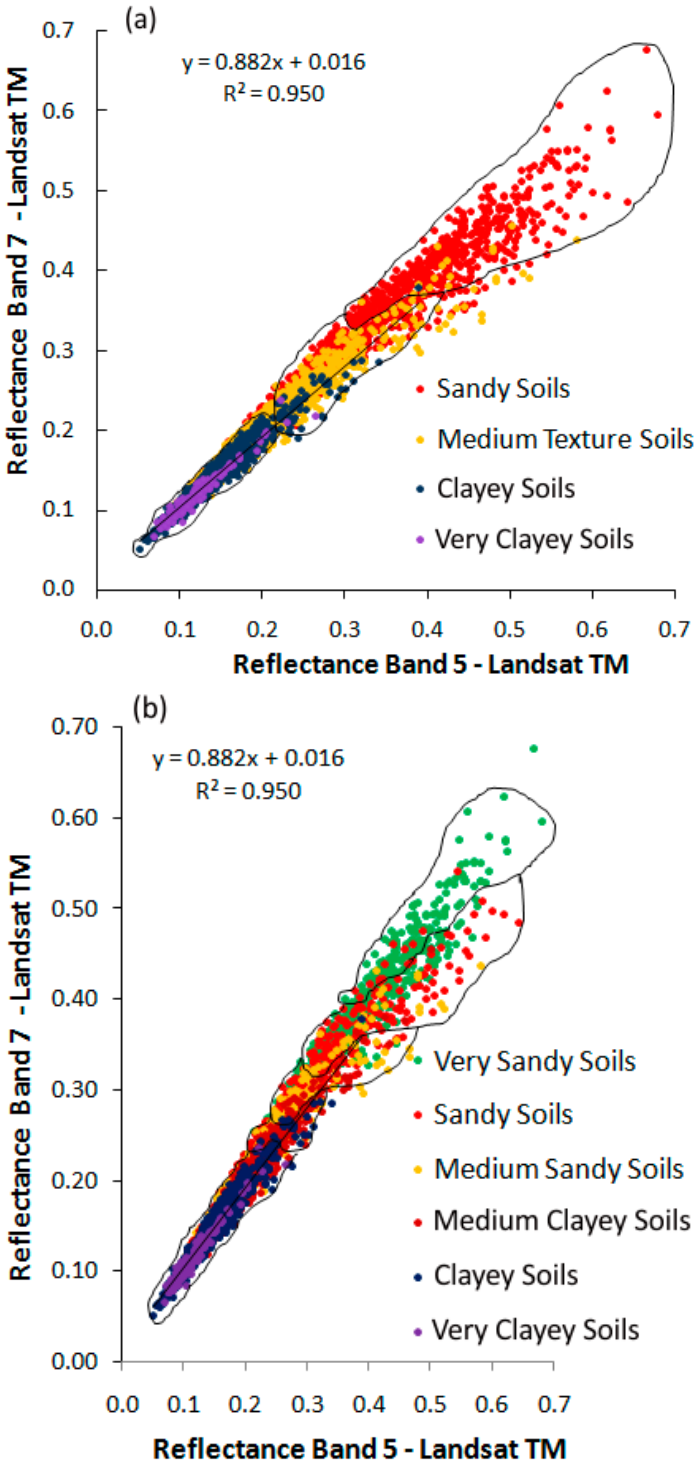

Figure 5. Soil lines obtained for the soils studied through laboratory data simulating the TM5 and TM7 bands: (**a**) distribution of textural classes according to the grouping for simplified classification according to SiBCS and (**b**) distribution of textural classes according to the LBTC.

Therefore, the XY graphs (band 5 vs. band 7) are represented better by the soil line than textural classes, since it represents soil constitution (Figure 5a,b). Indeed, band 5 also has an important relationship with quartz mineral.

Individualization of soil textural classes by means of spectroscopy at VIS-NIR-SWIR has been observed and reported by various authors and in Brazilian soils, such as Demattê and Garcia [6], Nanni

and Demattê [14], Ferraresi et al. [45], Vendrame et al. [46] and Franceschini et al. [36], among others. This individualization was corroborated in our study. On the other hand, the differentiated product obtained from this study was the distinguished individualization of textural soil classes according to the classification system adopted. The textural classification by management systems, which covered six classes, was the most suitable to plan sustainable agricultural activities.

3.2. Quantitative and Descriptive Spectral Assessment of the Soils Studied

3.2.1. Principal Component Analysis (PCA)

The results of the PCA are shown in Figure 6 through the chart of scores of PC1 vs. PC3, which constituted the PCs (Principal Components) with greater rates in the samples studied. PC1 represented 62% and PC3, 16% of the samples studied. The graph of scores showed that the spectral data were grouped according to their textural classes, represented by the PCA grouping.

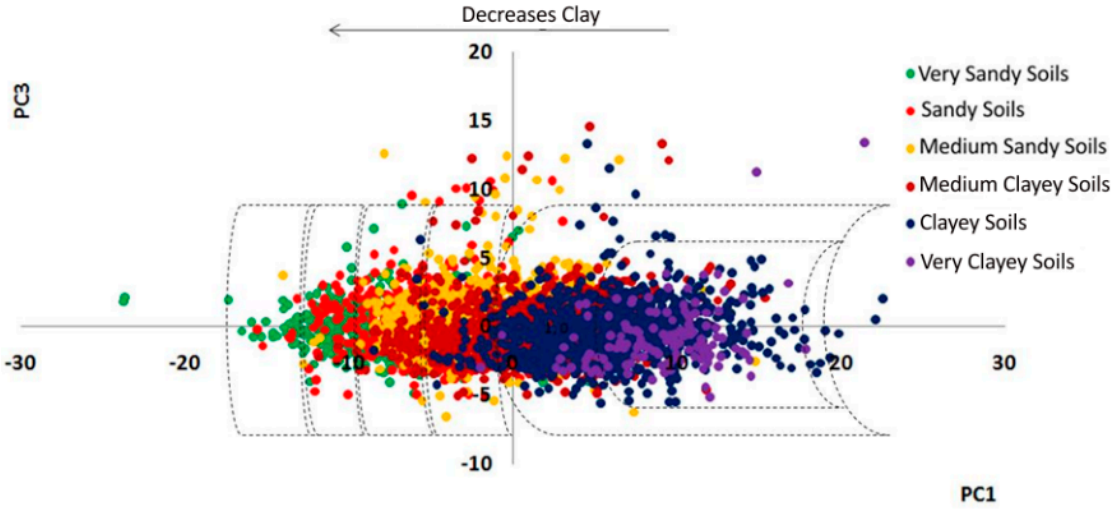

Figure 6. Scores chart of PC1 (Principal Component 1) vs. PC3 (Principal Component 3) showing the distribution of the studied soil samples, grouped by texture classes with sequential distribution along the spectrum.

The PCA dispersion presented sequential distribution of spectra of clayey and sandy classes, as reported by Sørensen and Dalsgaard [47], Ferraresi et al. [45] and Franceschini et al. [36]. Some points overlap between classes due to other soil attributes that influence the spectrum, such as OM and Fe oxides (Figure 6).

3.2.2. Prediction Models of Soil Attributes

The model that received Treatment 3 showed the best results for the quantification of sand and clay contents, reaching 0.93 and 0.96 of R^2, respectively (Figure 7a,b). The modeling procedure using absorbance of spectral data rather than reflectance proved to be more efficient, in agreement with Franceschini et al. [7,36] and Demattê et al. [31]. According to Sayes et al. [48], these R^2 indicate excellent quantitative models for prediction of soil attributes. Viscarra Rossel and McBratney [49] stated that the average value of R^2 for cross-validation of this attribute is about 0.76, using data at VIS-NIR wavelength. Viscarra-Rossel and Behrens [50] used several statistical algorithms and obtained R^2 between 0.88 and 0.77 for clay.

Treatment 3: PLSR3, transformation of spectral reflectance data to absorbance, reached RMSE (root mean square error) values of 83.8 for sand in the model calibration. Validation indicated that predictions could show a mean error of 8.38% in relation to the measured one. Stenberg et al. [36]

evaluated the results of 22 scientific works that were performed in different geographic regions and indicated an RMSE average of 5.7% for clay prediction. This value is lower than that found in this study. Viscarra-Rossel and Behrens [50] obtained RMSE 6.42% to 9.44% and only the latter value was higher than that obtained in this study. For sand prediction, RMSE was 132.7 in the calibration and 139.1 in the validation, which can be considered indicative of good performance (Figure 7a,b), according to Viscarra-Rossel and Behrens [50], R^2 also indicated good performance in agreement with Williams [51]. The performance of the model to predict clay and sand values is also demonstrated by the descriptive statistics presented in Table 1.

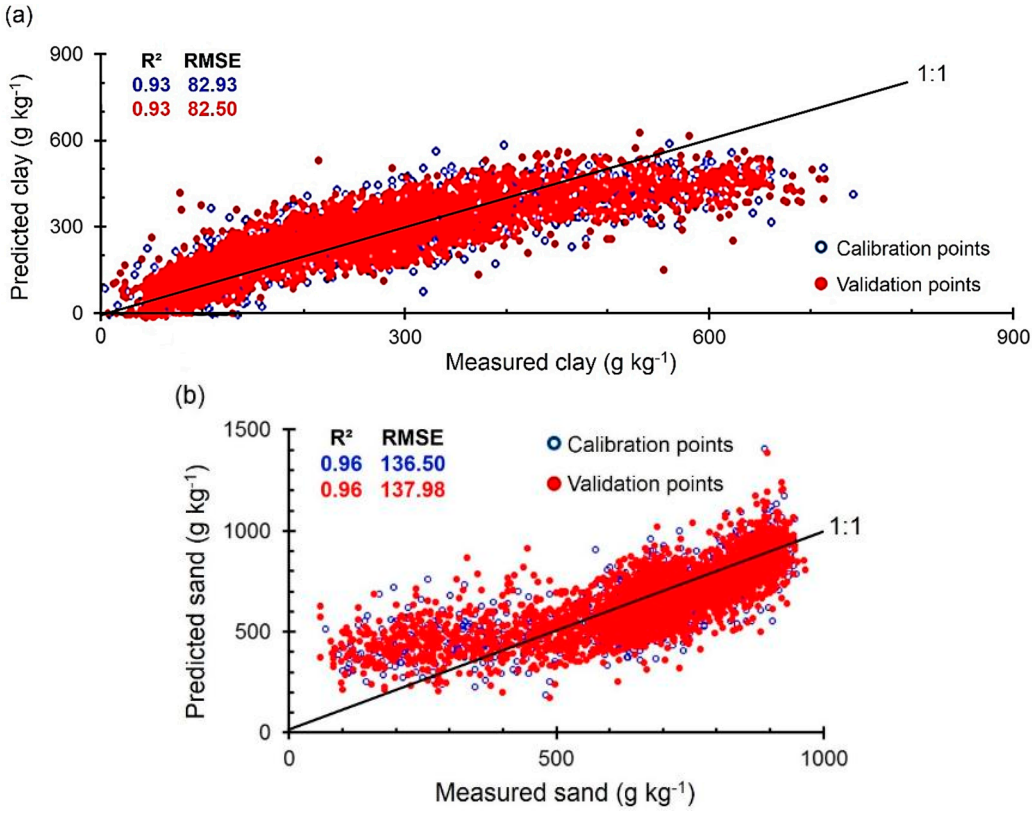

Figure 7. Regression results with Treatment 3: PLSR3, transformation of spectral reflectance data to absorbance, and generation of a prediction model for: clay (**a**); and sand (**b**).

The spectral bands that showed greater weight in clay quantification were at 516, 880, 995, 1117, 1413, 1874 and 2204 nm (Figure 2a,b). The band at 516 nm was related to Fe oxides [6] and bands at 1413 and 1874 nm referred to hygroscopic water retained by clay minerals [52,53]. In addition, we observed a feature related to kaolinite (2204 nm). Viscarra Rossel and Behrens [50] created prediction models for clay in Australian soils based on VIS-NIR spectrum and identified bands similar to those found in this study at 608, 988, 1392 and 2208 nm. The authors also considered important the wavelengths at 1908, 2184, 2236 and 2432 nm. Ben-Dor and Banin [54] obtained similar results and observed that the most important bands for clay calibration are related to hydroxyls and hygroscopic water, linked to Mg, Al and Fe in the crystal structure of clay minerals.

According to Chang et al. [35], 3.17 of RPD for clay shows excellent performance. Thus, the prediction for clay and sand content obtained in this study is compatible to those reported in other works. For instance, Shepherd and Walsh [10] and Viscarra-Rossel et al. [55] obtained R^2 0.85 and 0.78, with RMSE 75.0 g·kg^{-1} to predict clay content in soils of Africa and Australia, respectively. In studies conducted in Brazil, Demattê and Garcia [6] obtained R^2 0.90 for soils of Paraná State. Nanni and Demattê [14] obtained R^2 0.92 and 0.80 for clay and sand contents, respectively. Ferraresi et al. [45]

reached R^2 0.85 for clay content quantification and 0.87 for sand in São Paulo and Goiás States. In regional sampling of Latosols (Ferralsols) of the Brazilian Cerrado, Vendrame et al. [46] found 0.83 and 0.74 of R^2 for calibration and validation to determine clay content. In Mato Grosso do Sul State, Franceschini et al. [36] obtained satisfactory quantification for clay (R^2 = 0.92 and RPD = 3.59), silt (R^2 = 0.80 and RPD = 2.15) and sand (R^2 = 0.87 and RPD = 2.62). Therefore, quantification of clay, sand and silt contents by reflectance in VIS-NIR-SWIR spectroscopy can be considered an efficient methodology, provided there are controlled sampling and reliable analytical and spectral data arranged in a spectral library representative of soils in a given region.

Table 1. Descriptive statistical analysis for clay, silt and sand measured and predicted by elaborated quantification of these soil attributes model.

Statistical Parameters	Measured Values ($g \cdot kg^{-1}$)			Predicted Values ($g \cdot kg^{-1}$)		
	Clay	Silt	Sand	Clay	Silt	Sand
Average	274.49	69.86	655.65	272.06	73.12	654.82
Standard error	2.55	1.16	3.44	2.12	1.25	2.96
Median	260	45	691.5	274.22	75.81	645.16
Mode	280	40	680	341.88	146.19	1004
Standard deviation	155.99	70.86	210.71	130.01	76.66	181.3
Kurtosis	0.59	2.03	0.85	0.08	0.1	0.2
Asymmetry	740	592	909	830.66	1059.86	1424
Minimum	5	0	60	−189.4	−301.79	0
Maximum	745	504	969	641.26	758.07	1424
Coefficient of variation (%)	56.83	101.43	32.14	47.79	104.84	27.69

Descriptive statistical analyses were performed to assess contents of clay, silt and sand predicted by the quantification model that presented the best results of R^2 and RMSE, corresponding to the model with Treatment 3 in the spectral data. The average contents of clay, silt and sand in the two particle size compositions are very similar, with low values of standard error (Table 1).

The statistical parameters show the effectiveness of the generated prediction model for the clay content in Treatment 3 (Table 1). Observe that the measured and predicted clay were 274.49 and 272.06 $g \cdot kg^{-1}$, respectively, a very close match. The same occurred with silt and sand. The standard error was low, around 2. Cantarella et al. [56] studied variations between laboratory analyses and concluded that a range of 20% would be acceptable. Demattê et al. [57] used this type of comparison between laboratory and spectroscopy measurements and concluded that most results were within the indicated range. In the present study, the difference in the case of clay was 1.2%, thus within the 20% range (Table 1). These indicate that the models reached very close results to laboratory information.

3.2.3. Ternary Diagrams of Textural Classification of Soils: Real vs. Spectral Values

Ternary diagrams were performed for the soil textural evaluation (Figure 8a, measured values; and Figure 8b, predicted values). Sand and clay were determined by spectra as silt by their difference and inserted in the diagrams. The assessment of predicted values was performed by Treatment 3 (regression of 0.93 and 0.96 for clay and sand, respectively). We observed similarity of samples distribution and their corresponding textural classes (Figure 8a,b). Most similarity is concentrated for sandy soils moving towards clayey ones.

On the other hand, laboratory measurements presented some slight differences on path distribution of the ternary graphic (Figure 8a,b). When we reach about 50% of clay, seems that predicted values did not attempt to the measured ones, and spectra can be underestimating values at these texture classifications. This matches with statistical observation at Figure 7a. Clayey soils from these areas have greater amount of ilmenite and magnetite, since are developed from basaltic rocks. These components occur in soil sand and silt fraction, and have very low spectra because absorbs energy (Figure 8c). A possible explanation would be that over certain value of clay (about

500 g·kg^{-1}, 50%), the spectra starts to be extremely similar, because of saturation, and the spectra diminish its sensitivity. In fact, Figures 2b and 4a show this similarity. Indeed, Figure 6 shows a strong overlap between the spectra of these two textural classes on soil line, as well. Thus, spectra can have lower sensitivity on the quantification of soils with these mineralogies, when have high values of clay. A stronger evidence of this fact is corroborated by Cezar et al. [58]. These authors observed that small amounts of magnetite can masks other components. Figure 8c illustrate magnetite spectra as compared with a clayey soil with opaque mineral.

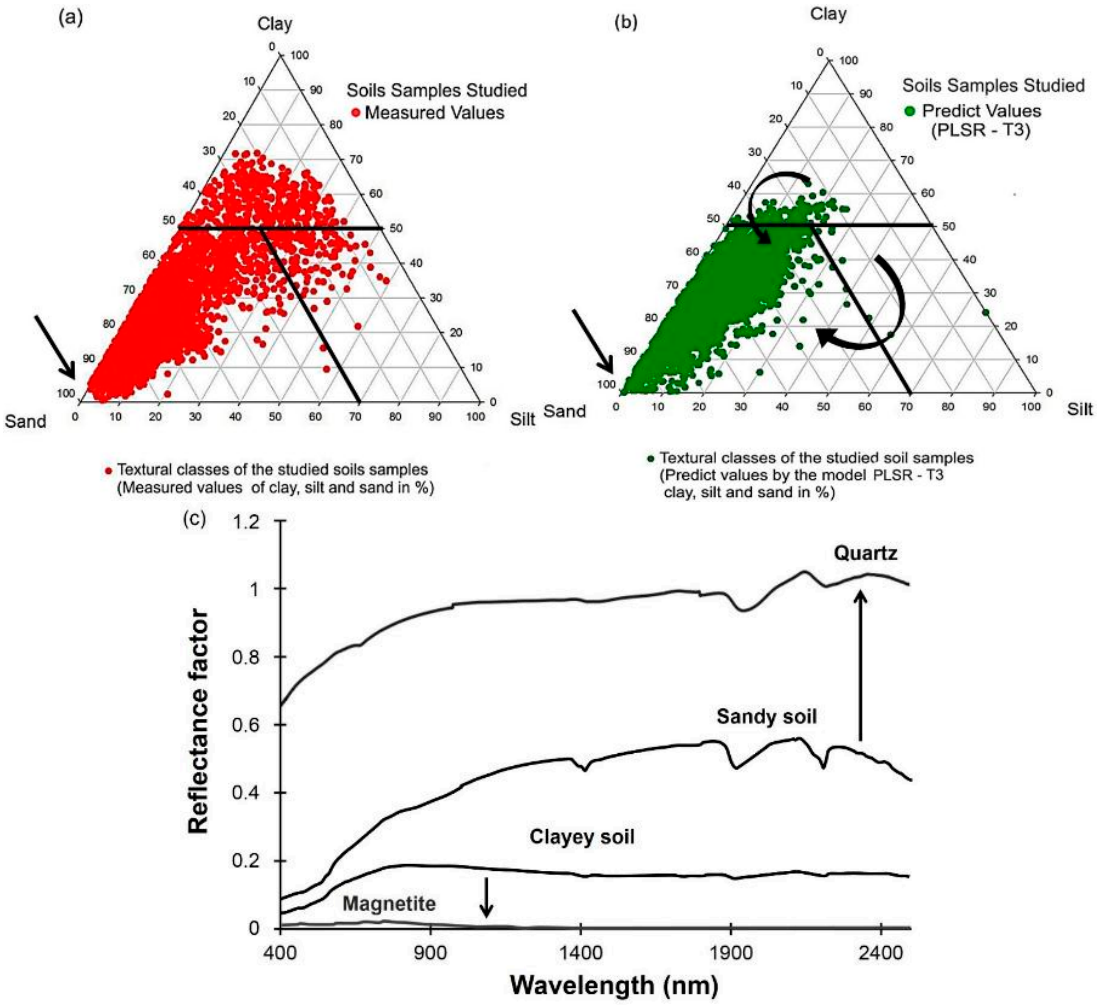

Figure 8. Ternary diagram of soils textural classification: (**a**) clay, silt and sand measured; (**b**) clay, silt and sand predicted by the model with Treatment 3; and (**c**) representative spectral curves (Adapted from Cezar et al. [58]).

In addition, we observe that for very sandy samples happened the opposite (Figure 8a,b). Many observations were overestimated when are very sandy, which also has support from the model presented at Figure 7b. Thus, predicted values filled the corner of sandy texture (when values of sand goes higher, plots goes 'down' in the graphic). If on one hand the area has soils developed by basalt, on the other hand, we have sandstone as well. In this case, samples with high amount of quartz, which has high reflectance (Figure 8c) can improve saturation on reflection. Figure 8c illustrate quartz spectra as compared with a sandy soil. Silt was calculated as the difference of predicted sand and clay, and shifted its position in the figure. These are the first findings in this matter. Thus, despite these possibilities, we state the necessity of new evaluations of spectral quantification of very clayey and very sandy soils with this mineralogy.

3.3. Soil Spectral Classification by Textural Information

We inserted into the LDA, the spectra of both depths (respective to horizons, A and B) of each observation, classified as Ferralsols (LV), Lixisols (PV) and Arenosols (RQ) (Figure 9a). Each soil unit (i.e., Ferralsols and Lixisols) can have different textures and are presented in Figure 9b,c. The objectives of these analyses are: (a) to distinguish soil classes; and (b) to distinguish soil classes in function of their textural class. The discrimination of soil classes indicated 73%, 66% and 78% accuracy, mainly in the linear combination 1 (LD_1: 94.60%; 99.78%; and 98.75%), respectively (Figure 9). On the other hand, LD_2 (5.4%) indicated the distinction for PV (Lixisols) and the other two classes (Figure 9a).

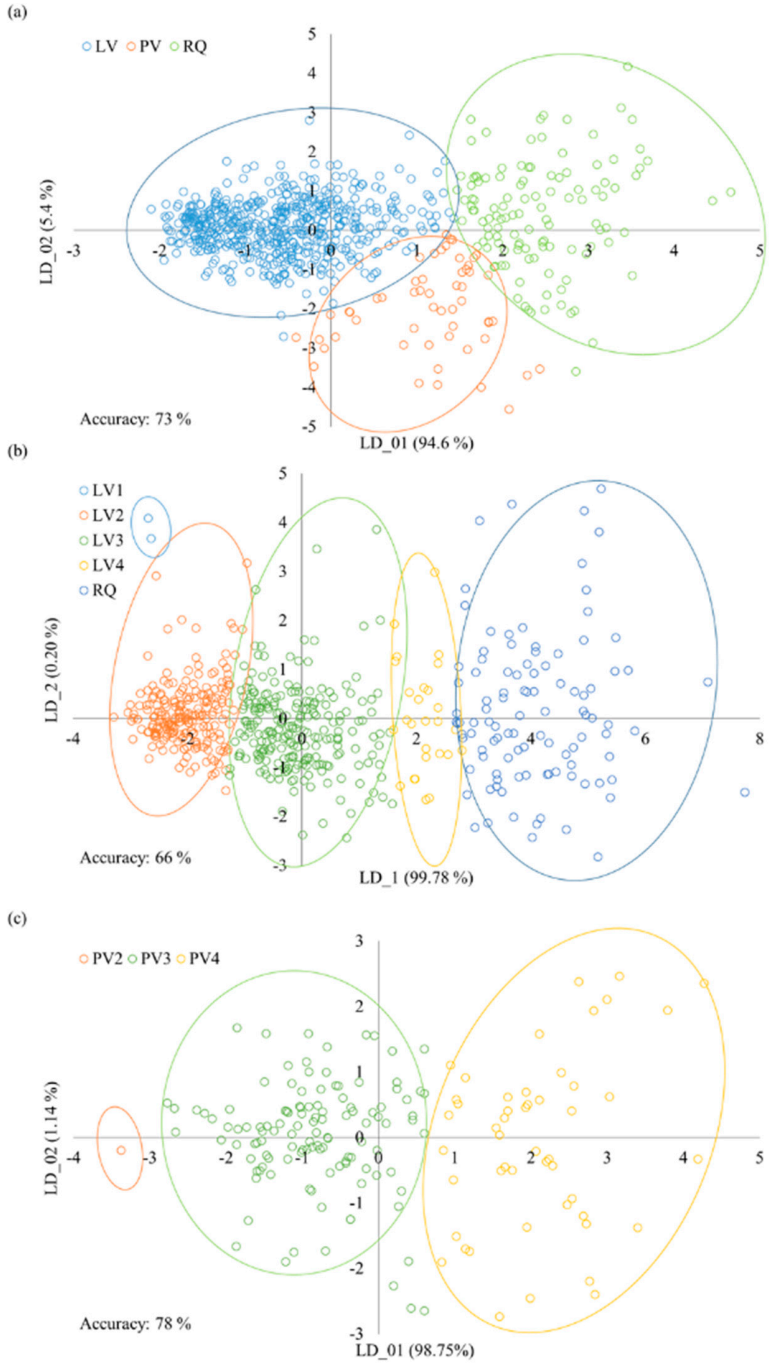

Figure 9. Predicted discrimination among: (**a**) Ferralsols (LV), Lixisols (PV) and Arenosols (RQ); (**b**) Ferralsols with different textures and Arenosols; and (**c**) Lixisols with diferrent textures.

In general, the principal components 2 (PC_2) and 3 (PC_3) are more related with the ratio between visible and NIR regions [55]. The confusion between soil classes can occur when we have the same class with different textures, but near the border of the texture limit. This is due to the inherent subjectivity on the establishment of limits of the textural classes. Indeed, texture is an important primary property that defines the reflectance intensity of soil classes.

The results in Figure 9a indicate a great discrimination between soil classes. This was possible because we inserted, into the same matrix, the spectra of horizons A and B, respectively, from each observation. As a matter of taxonomic classification, Ferralsols do not have significant differences between clay contents in the horizons. On the other hand, Lixisols have great textural differentiation between horizons. As described by Demattê et al. [31], these differences can clearly be seen mostly after 1500 nm, where A horizon presents a stronger reflection (due to the influence of higher quartz content) than on horizon B (with lower quartz content). Ferralsols have similar clay contents between horizons A and B, and, thus, the spectra are similar. When statistics compared these two soil classes simultaneously, the difference could be detected.

Figure 9b shows a different site. Although Ferralsols (LV) have similar clay contents between horizons, the content could be differentiated as very clayey (LV1), clayey (LV2), loam clay (LV3) and loam sandy (LV4). Thus, we observed that spectroscopy could discriminate the different types of Ferralsols in terms of texture classification. When textures in both horizons are sandy, the taxonomic name is no longer Ferralsol, but Arenosol. The textures in both horizons of Arenosols were sandy and well discriminated from Ferralsols. We can observe the important proportion of discrimination from LV1-LV2-LV3-LV4-RQ, in the same sequence of clay content. Figure 9c shows the same great discrimination between PV with variation in the clay content between depths. In this case, we did not have PV1 (very clayey), but PV2, PV3 and PV4 were well differentiated.

4. Conclusions

1. The regional soil spectral library showed that sandy soils have a higher reflectance intensity than clayey ones. From sandy to clayey soils, there is an angular upward variation from VIS-NIR to SWIR (greater in SWIR). This fact is attributed to OM and Fe oxides that absorb energy in VIS-NIR and quartz that increases the reflectance in SWIR. Textural classes show a logical series of increased reflectance from very clayey < clayey < medium-clayey < medium-sandy < sandy < very sandy.

2. The spectral response of the studied soils were resampled to bands 3, 4, 5 and 7 of Landsat. The relationship between bands 3/4 show angular variation from clayey to sandy soils. The ratio of bands 5 and 7, in turn, cause intensity variation instead. Therefore, the descriptive evaluation of spectral curves detected differences between textural classes.

3. It was possible to quantify the clay and sand contents in a wide population of samples reaching R^2 = 0.93 and 0.96 with low RMSE. The results were also compared with laboratory measurements, and placed into the acceptable range of its variancy. Indeed, we reached a 1.2% difference between laboratory and spectroscopy measurement for clay. The best spectral processing method was that done in Treatment 3.

4. The textural classification with four classes in accordance with the simplified classification of SiBCS and that used in Land Use and Management Brazilian Technical Classifications with six classes were well discriminated by the spectral curves. This is important because it indicates the sensibility of spectroscopy to distinguish detailed soil texture classes (mostly the medium to sandy textures) as well as to help pedology and soil management.

5. The ternary classification using particle size classes obtained by spectroscopy was very similar to the particle size analysis carried out in the laboratory. On the other hand, it seems that soil samples over about 50% clay content have been, in general, underestimated. This can be possible on the case of clayey soils with high opaque minerals. For samples with high contents of sand, the opposite occurred. These are the first findings in this matter. Thus, we state the necessity of new evaluations of spectral quantification of very clayey and very sandy soils with this mineralogy.

6. The results show that spectroscopy may be used to measure the soil particle size, however, it depends on laboratory standards, analyses and statistical modeling.

7. Spectroscopy was able to discriminate soil classes such as Ferralsols, Arenosols and Lixisols. Despite this, spectra was able to indicate in what texture each soil class belong. Thus, discrimination of the same soil class, and its texture class variancies, in specific for Ferralsols and Arenosols, could be characterized.

Acknowledgments: The authors gratefully acknowledge the financial support of CAPES, CNPQ and FAPESP and Department of Soil Science of ESALQ-USP in carrying out the analysis. This work is part of the post-doctoral studies of the first author who expresses her thanks to José Alexandre Demattê of LSO-ESALQ-USP for his guidance, to the team GeoCis group and to the University of Brasilia for granting permission for the completion of the post-doctoral program.

Author Contributions: The study was conducted by Marilusa P. C. Lacerda developed for her post-doctoral studies under the guidance of José Alexandre M. Demattê. Marcus V. Sato and Arnaldo B. Souza collaborated in carrying out the statistical analysis and Caio T. Fongaro and Bruna C. Gallo organized the database. All read and reviewed the article.

Conflicts of Interest: The authors declare no conflict of interest.

References

1. Demattê, J.L.I.; Demattê, J.A.M. Environment productivity as a strategy for sugar cane culture. *Inform. Agron.* **2009**, *127*, 10–18.
2. Mendonça-Santos, M.L.; Santos dos, H.G. The state of the art of Brazilian soil mapping and prospects for digital soil mapping. In *Digital Soil Mapping An Introductory Perspective*; Lagacherie, P., McBratney, A.B., Voltz, B.T., Eds.; Elsevier: Amsterdam, The Netherlands, 2006; pp. 39–54.
3. Camargo, M.N.; Klant, E.; Kauffman, J.H. Classificação de solos usada em levantamentos pedológicos no Brasil. *Soc. Bras. Ciênc. Solo* **1987**, *12*, 11–13.
4. Embrapa—Empresa Brasileira de Pesquisa Agropecuária. *Sistema Brasileiro de Classificação de Solos*, 3rd ed.; Centro Nacional de Pesquisa de Solos, Embrapa: Brasília, Brazil, 2013.
5. FAO—Food and Agriculture Organization of United Nations. *World Reference Base for Soil Resources*; FAO/International Soil Reference and Information Centre-ISRIC/International Union of Soil Sciences-IUSS: New York, NY, USA, 2006.
6. Demattê, J.A.M.; Garcia, G.J. Avaliação de atributos de latossolo bruno e de Terra bruna estruturada da região de Guarapuava, Paraná, por meio de sua energia refletida. *Rev. Bras. Ciênc. Solo* **1999**, *23*, 343–355. [CrossRef]
7. Franceschini, M.H.D.; Demattê, J.A.M.; da Terra, F.S.; Vicente, L.E.; Bartholomeus, H.; Souza Filho, C.R. Prediction of soil properties using imaging spectroscopy: Considering fractional vegetation cover to improve accuracy. *Int. J. Appl. Earth Obs. Geoinf.* **2015**, *38*, 358–370. [CrossRef]
8. Dalmolin, R.S.D.; Gonçalves, C.N.; Klamt, E.; Dick, D.P. Relação entre os constituintes do solo e seu comportamento espectral. *Cienc. Rural* **2005**, *35*, 481–489. [CrossRef]
9. Terra, F.S.; Demattê, J.A.M.; Viscarra-Rossel, R.A. Spectral libraries for quantitative analyses of tropical Brazilian soils: Comparing vis–NIR and mid-IR reflectance data. *Geoderma* **2015**, *255–256*, 81–93. [CrossRef]
10. Shepherd, K.D.; Walsh, M.G. Development of reflectance spectral libraries for characterization of soil properties. *Soil Sci. Soc. Am. J.* **2002**, *66*, 988–998. [CrossRef]
11. Ben-Dor, E. Quantitative remote sensing of soil properties. *Adv. Agron.* **2002**, *75*, 173–243.
12. Dunn, B.W.; Beecher, H.G.; Batten, G.D.; Ciavarella, S. The potential of near-infrared reflectance spectroscopy for soil analysis—A case study from the Riverine Plain of south-eastern Australia. *Aust. J. Exp. Agric.* **2002**, *42*, 607–614. [CrossRef]
13. Viscarra-Rossel, R.A.; Walvoort, D.J.J.; Mcbratney, A.B.; Janik, L.J.; Skjemstad, J.O. Visible, near infrared, mid infrared or combined diffuse reflectance spectroscopy for simultaneous assessment of various soil properties. *Geoderma* **2006**, *131*, 59–75. [CrossRef]
14. Nanni, M.R.; Demattê, J.A.M. Spectral reflectance methodology in comparison to traditional soil analysis. *Soil Sci. Soc. Am. J.* **2006**, *70*, 393–407. [CrossRef]

15. Brown, D.J.; Shepherd, M.G.W.; Walsh, M.G.; Mays, M.D.; Reinsch, T.G. Global soil characterization with VNIR diffuse reflectance spectroscopy. *Geoderma* **2006**, *132*, 273–290. [CrossRef]
16. Maleki, M.R.; Mouazen, A.M.; Ramon, H.; de Baerdemaeker, J. Optimization of soil VIS-NIR sensor-based variable rate application system of soil phosphorus. *Soil Tillage Res.* **2007**, *94*, 239–250. [CrossRef]
17. Mouazen, A.M.; Maleki, M.R.; de Baerdemaeker, J.; Ramon, H. On-line measurement of some selected soil properties using a VIS–NIR sensor. *Soil Tillage Res.* **2007**, *93*, 13–27. [CrossRef]
18. Summers, D.; Lewis, M.; Ostendorf, B.; Chittleborough, D. Visible near-infrared reflectance spectroscopy as a predictive indicator of soil properties. *Ecol. Indic.* **2009**. [CrossRef]
19. Soriano-Disla, J.M.; Janik, J.; Viscarra-Rossel, R.A.; Macdonald, L.M.; McLaughlin, M.J. The performance of visible, near, and mid-infrared reflectance spectroscopy for prediction of soil physical, chemical, and biological properties. *Appl. Spectrosc. Rev.* **2014**, *49*, 139–186. [CrossRef]
20. Bellinaso, H.; Demattê, J.A.M.; Araújo, S.R. Soil spectral library and its use in soil classification. *Rev. Bras. Ciênc. Solo* **2010**, *34*, 861–870. [CrossRef]
21. Van Reeuwjik, L.P. *Procedure for Soil Analysis*, 6th ed.; ISRIC: New York, NY, USA, 2002.
22. Viscarra Rossel, R.A.; Webster, R. Predicting soil properties from the Australian soil visible near infrared spectroscopic database. *Eur. J. Soil Sci.* **2012**, *63*, 848–860. [CrossRef]
23. USDA—United States Department of Agriculture. *Rapid Carbon Assessment (RaCA) Methodology*; NRCS/USDA: New York, NY, USA, 2013.
24. Stevens, A.; Nocita, M.; Toth, G.; Montanarella, L.; van Wesemael, B. Prediction of soil organic carbon at the European scale by visible and near infrared reflectance spectroscopy. *PLoS ONE* **2013**, *8*. [CrossRef]
25. Nocita, M.; Stevens, A.; van Wesemael, B.; Aitkenhead, M.; Bachmann, M.; Barthès, B.; Ben dor, E.; Brown, D.J.; Clairotte, M.; Csorba, A.; et al. Soil spectroscopy: An alternative to wet chemistry for soil monitoring. In *Advances in Agronomy*; Sparks, D.L., Ed.; Academic Press: New York, NY, USA, 2015; pp. 139–159.
26. Embrapa—Empresa Brasileira de Pesquisa Agropecuária, Centro Nacional de Pesquisas de Solos. *Manual de Métodos de Análise de Solos*, 2nd ed.; Embrapa: Rio de Janeiro, Brasil, 1997.
27. Chicati, M.L.; Nanni, R.; Cézar, E.; Oliveira, R.B.; Demattê, J.A.M. Análise comparativa da determinação da linha dos solos em área de várzea nos níveis orbital e laboratorial. In Proceedings of the XVI Simpósio Brasileiro de Sensoriamento Remoto, Foz do Iguaçu, Brazil, 13–18 April 2013.
28. Huete, A.R. Soil influences in remotely sensed vegetation canopy spectra. In *Theory and Application of Optical Remote Sensing*; Asrar, G., Ed.; Wiley Interscience: New York, NY, USA, 1989; pp. 107–141.
29. Fukuhara, M.; Hayasiu, S.; Yasuda, Y. Extraction of soil information from vegetated areas. In Proceedings of the Machine Processing of the Remotely Sensed Data, West Lafayette, IN, USA, 27–29 June 1979.
30. Demattê, J.A.M. Characterization and discrimination of soils by their reflected electromagnetic energy. *Braz. J. Agric. Res.* **2002**, *37*, 1445–1458. [CrossRef]
31. Demattê, J.A.M.; Bellinaso, H.; Romero, D.J.; Fongaro, C.T. Morphological Interpretation of Reflectance Spectrum (MIRS) using libraries looking towards soil classification. *Sci. Agric.* **2014**, *71*, 509–520. [CrossRef]
32. CAMO A/S. *The Unscrambler User's Guide*; CAMO: Trondheim, Norway, 1998.
33. Wold, H. *Systems under Indirect Observation*; Elsevier: Amsterdam, The Netherlands, 1982.
34. Campbell, N.A.; Mulcahy, M.J.; Mcarthur, W.M. Numerical classification of soil profiles on the basis of field morphological properties. *J. Soil Res.* **1970**, *8*, 43–58. [CrossRef]
35. Chang, C.W.; Laird, D.A.; Mausbach, M.J.; Hurburgh Junior, C.R. Near-infrared reflectance spectroscopy—Principal components regression analyses of soil properties. *Soil Sci. Soc. Am. J.* **2001**, *65*, 480–490. [CrossRef]
36. Franceschini, M.H.D.; Demattê, J.A.M.; Sato, M.V.; Vicente, L.E; Grego, C.R. Abordagens semiquantitativa e quantitativa na avaliação da textura do solo por espectroscopia de reflectância bidirecional no VIS-NIR-SWIR. *Pesqui. Agropecu. Bras.* **2013**, *48*, 1568–1581. [CrossRef]
37. Stenberg, B.; Viscarra-Rossel, R.A.; Mouazen, A.M.; Wetterlind, J. Visible and near infrared spectroscopy in soil science. In *Advances in Agronomy*; Sparks, D.L., Ed.; Academic Press: Burlington, ON, Canada, 2010; pp. 163–215.
38. Fisher, R. The use of multiple measurements in taxonomic problems. *Ann. Hum. Genet.* **1936**, *7*, 179–188. [CrossRef]
39. R Core Team. *R: A Language and Environment for Statistical Computing*; The R Foundation for Statistical Computing: Vienna, Austria, 2016.

40. Almeida, F.F.M.; Barbosa, O. *Geologia das Quadrículas de Piracicaba e Rio Claro, Estado de São Paulo*; Departamento Nacional de Pesquisa Mineral/Divisão de Geologia Mineral: Rio de Janeiro, Brazil, 1953.
41. Stoner, E.R.; Baumgardner, M.F. Characteristics variations in reflectance of surface soils. *Soil Sci. Soc. Am. J.* **1981**, *45*, 1161–1165. [CrossRef]
42. Baret, F.; Jacquemound, S.; Hanoq, J.F. The soil line concept in remote sensing. *Remote Sens. Environ.* **1983**, *7*, 1–18. [CrossRef]
43. Nanni, M.R.; Demattê, J.A.M. Quantification and discrimination of soils developed from basalt as evaluated by terrestrial, airborne and orbital sensors (Compact Disc). In Proceedings of the X Simpósio Brasileiro de Sensoriamento Remoto, Foz do Iguaçu, Brazil, 21–26 April 2001.
44. Nanni, M.R.; Demattê, J.A.M. Comportamento da linha do solo obtida por espectrorradiometria laboratorial para diferentes classes de solo. *Rev. Bras. Ciênc. Solo* **2006**, *30*, 1031–1038. [CrossRef]
45. Ferraresi, T.M.; da Silva, W.T.L.; Martin-Neto, L.; da Silveira, P.M.; Madari, B.E. Espectroscopia de infravermelho na determinação da textura do solo. *Rev. Bras. Ciênc. Solo* **2012**, *36*, 1769–1777. [CrossRef]
46. Vendrame, P.R.S.; Marchão, R.L.; Brunet, D.; Becquer, T. The potential of NIR spectroscopy to predict soil texture and mineralogy in Cerrado Latosols. *Eur. J. Soil Sci.* **2012**, *63*, 743–753. [CrossRef]
47. Sørensen, L.K.; Dalsgaard, S. Determination of clay and other soil properties by near infrared spectroscopy. *Soil Sci. Soc. Am. J.* **2005**, *69*, 159–167. [CrossRef]
48. Sayes, W.; Mouazen, A.M.; Ramon, H. Potential for onsite and online analysis of pig manure using visible and near infrared reflectance spectroscopy. *BIOS Engl.* **2005**, *91*, 393–402. [CrossRef]
49. Viscarra-Rossel, R.A.; Mcbratney, A.B. Diffuse reflectance spectroscopy as a tool for digital soil mapping. In *Digital Soil Mapping with Limited Data*; Hartemink, A.E., McBratney, A.B., Mendonça-Santos, L., Eds.; Springer Netherlands: Dordrecht, The Netherlands, 2008; pp. 165–172.
50. Viscarra-Rossel, R.A.; Behrens, T. Using data mining to model and interpret soil diffuse reflectance spectra. *Geoderma* **2010**, *158*, 46–54. [CrossRef]
51. Williams, P.C. Implementation of near infrared technology. In *Near Infrared Technology in the Agricultural and Food Industries*; American Association of Cereal Chemists: Eagan, MN, USA, 2001; pp. 145–169.
52. Lindberg, J.D.; Snyder, D.G. Diffuse reflectance spectra of several clay minerals. *Am. Mineral.* **1972**, *57*, 485–493.
53. Hunt, G.R. Near-infrared (1.3–2.5 μm) spectra of alteration minerals—Potential for use in remote sensing. *Geophysics* **1979**, *44*, 1974–1986. [CrossRef]
54. Ben-Dor, E.; Banin, A. Near-infrared reflectance analysis of carbonate concentration in soils. *Appl. Spectrosc.* **1990**, *44*, 1064–1069. [CrossRef]
55. Viscarra-Rossel, R.A.; Cattle, S.R.; Ortega, A.; Fouad, Y. In situ measurements of soil color, mineral composition and clay content by Vis–NIR spectroscopy. *Geoderma* **2009**, *150*, 253–266. [CrossRef]
56. Cantarella, H.; Quaggio, J.A.; van Raij, B.; Abreu, M.F. Variability of soil analysis of commercial laboratories: Implications for lime and fertilizer recommendations. *Commun. Soil Sci. Plant Anal.* **2006**, *37*, 2213–2225. [CrossRef]
57. Demattê, J.A.M.; Fiorio, P.R.; Araujo, P.R. Variation of routine soil analysis when compared with hyperspectral narrow band sensing method. *Remote Sens.* **2010**, *2*, 1998–2016. [CrossRef]
58. Cezar, E.; Nanni, M.R.; Chicati, M.L.; Souza Júnior, I.G.; Costa, A.C.S. Use of spectral data for estimating the relationship between iron oxides and 2:1 minerals with their respective reflectances. *Semin. Ciênc. Agrár.* **2013**, *34*, 1479–1492.